Volume 9, Number 2
1009-1963/2000/09(02)/0141-08
CHINESE PHYSICS
February, 2000
© 2000 Chin. Phys. Soc.

SIMULATION ON LOCAL FLUX CREEP IN TYPE-Ⅱ SUPERCONDUCTORS*

Nie Hui-fen(聂惠芬), Liu Yu-feng(刘宇峰), Huang Yi-mei,(黄奕梅),
and Yan Shou-sheng(阎守胜)

Department of Physics, Peking University, Beijing 100871, *China*

(Received 3 August 1999; revised manuscript received 9 September 1999)

Using C programming language, we have simulated the flux creep process in nonideal type-Ⅱ superconductors. Global and local magnetization curves are calculated and the logarithmic time dependence of local magnetic induction B under a constant external field is examined. The effects of nonuniform pinning potential and self-organized criticality (SOC) model on the simulations are discussed. The results show that the main feature of flux creep is the relaxation effect. The form of hysteresis loops is dependent on the magnetic field sweep rate. SOC can account for the occurrence of fluctuation to a certain extent and nonuniform pinning potential can enhance the fluctuation.

PACC: 7460G; 7560; 7440

I. INTRODUCTION

Thermally activated flux creep in high-temperature superconductors(HTS) has been a hot spot in the field of superconductivity. The traditional way to investigate this phenomenon is to measure the time dependence of the magnetic moment averaged over the whole sample and then extract from the data such important parameters as the effective energy U and the logarithmic time scale t_0.[1] In the area of theoretical research, Anderson first put forward the concept of thermally activated flux creep and presented a phenomenological model. His theory predicted that the magnetic moment should decay linearly in $\log(t)$, where t is the time, and this prediction was confirmed by experiments.[2] However, subsequent researches showed that Anderson-Kim (A-K) model cannot fully explain the relaxation process in HTS and thus necessitated the introduction of new models, which emphasize the nonlinear dependence of U on the current density J.[3,4] Since it is not possible to derive $U(J)$ directly from experimental data, each of the above models gives a specific relaxation behavior that can be compared with experimental results. Such an approach for evaluating $U(J)$ is model-dependent and involves fitting several parameters.[5]

Employing an array of micro Hall probes, Zeldov et al.[6] measured the spatial distribution and time dependence of the magnetic induction in YBCO crystals, then analyzed the data on the basis of flux diffusion equations,[7,8] which allowed a direct, model-independent determination of the local activation energy U. Their experimental results clearly exhibited the nonuniformity of local relaxation.[9] And subsequent similar work all disclosed important information that were hidden in global measurements. Another approach for studying flux dynamics is through computer simulation.[10] From simulations on superconducting vortices, Richarson et al.[11] confirmed a modified Bean model for the magnetization of hard type-Ⅱ superconductors and suggested the likely existence of self-organized criticality (SOC) mechanism in the dynamics of vortices. In this work, we simulate the flux creep in type-Ⅱ superconductors. We examine global and local hysteresis loops and the logarithmic time dependence of local magnetic induction B under a constant external field and thus obtain a clear view of the flux penetration process at different locations within the sample. We also investigate the dependence of local hysteresis loops on the magnetic field sweep rate. Finally, we discuss the effects of nonuniform pinning potentials and SOC model on the flux creep simulation.

Ⅱ. PRINCIPLE AND MODEL

In ideal type-Ⅱ superconductors where there are no material inhomogenieties, the only force acting on flux lines in the mixed state is the interaction between them. In the presence of field gradient, flux lines move opposite to the direction of the gradient. Whereas in nonideal type-Ⅱ superconductors, the balance between the pinning force arising from material inhomogenieties and the electromagnetic driving force determines the movement of the flux lines. We use $\boldsymbol{F}_{\rm d}$ to represent the driving force, $\boldsymbol{F}_{\rm p}$ the pinning force. At absolute

* Project supported by the National Center for Research & Development on Superconductivity of China.

zero temperature, in the critical state one has

$$\boldsymbol{F}_{\rm d} + \boldsymbol{F}_{\rm p} = 0. \tag{1}$$

The expression for the driving force density is Lorentz-like

$$\boldsymbol{F}_{\rm d} = \boldsymbol{J} \times \boldsymbol{B}, \tag{2}$$

where $\boldsymbol{J}$ is the current density near the flux line. From Eq.(1) one can derive the largest persistent current density, i.e., the critical current density $\boldsymbol{J}_{\rm c}$,

$$\boldsymbol{F}_{\rm p} = \boldsymbol{J}_{\rm c} \times \boldsymbol{B}. \tag{3}$$

According to the critical-state model, at $T = 0$ the fluxoids in the bulk of a hard superconductors can move only if the driving force density $\boldsymbol{F}_{\rm d}$ acting on them exceeds the maximum local pinning force density $\boldsymbol{F}_{\rm p}$. Due to the complexity of the factors determining the pinning force density, it is very difficult to describe flux pinning only from the critical state conditions. Bean and Livingston[12] put forward a simplified model which assumes the critical current density $\boldsymbol{J}_{\rm c}$ to be constant.

The critical state discussed above is a metastable one. At nonzero temperature, flux creep is possible with the help of thermal activation even if $\boldsymbol{F}_{\rm d} < \boldsymbol{F}_{\rm p}$, thus causing the metastable state to break down. According to Anderson's theory of flux creep, the rate at which flux lines jump over the pinning barriers is given by the usual Arrhenius expression

$$\omega_{\rm r} = \omega_0 {\rm e}^{-U/k_{\rm B}T} = \omega_0 {\rm e}^{-(U_0 - U_{\rm d})/k_{\rm B}T}, \tag{4}$$

where ω_0 is an attempt frequency and $U = U_0 - U_{\rm d}$ is an effective activation energy. Here U_0 is the effective height of the energy barrier that arises from material inhomogenieties, $U_{\rm d}$ is the decrease in the height of the barrier due to the work done by the driving force. Assume U_0 is identical for each pinning center, the rate at which flux lines jump back from the neighbouring site is

$$\omega_{\rm r} = \omega_0 {\rm e}^{-U/k_{\rm B}T} = \omega_0 {\rm e}^{-(U_0 + U_{\rm d})/k_{\rm B}T}. \tag{5}$$

Considering the flux-motion equation

$$\frac{\partial \boldsymbol{B}}{\partial t} = -\nabla \times (\boldsymbol{B} \times \boldsymbol{v}), \tag{6}$$

the simplest relation between the drift velocity $\boldsymbol{v}$ of vortices and the activation energy U is

$$\boldsymbol{v} = \boldsymbol{v}_0 \exp\left[-\frac{U}{k_{\rm B}T}\right]. \tag{7}$$

When there is no external field, the pining potential is not periodic because of the random distribution of pinning centers in the sample. From a given site i, a vortex can jump to the left site $(i-1)$ or the right site $(i+1)$,and from these sites the vortex can jump back into site i. The jump rate due to thermal activation for hopping from site i to site j is proportional to $B_i \exp(-U_{ij}/k_{\rm B}T)$. Then from the law of conservation of the number of vortices, one can get

$$\begin{aligned} B_i((n+1)\Delta t) = B_i(n\Delta t) + \frac{1}{2}\omega_0 \Delta t \\ \times [-B_i(n\Delta t){\rm e}^{-\varepsilon_{i,j+1}} - B_i(n\Delta t){\rm e}^{-\varepsilon_{i,i-1}} \\ + B_{i+1}(n\Delta t){\rm e}^{-\varepsilon_{i+1,i}} + B_{i-1}(n\Delta t){\rm e}^{-\varepsilon_{i-1,i}}], \end{aligned} \tag{8}$$

where $\varepsilon_{i,j} = U_{i,j}/k_{\rm B}T$, ω_0 is the microscopic attempt frequency to jump out of a given site. This equation serves as the basis for our computer simulation on the thermally-activated process. For the sake of comparison, we take $\omega_0 = 4 \times 10^5\,{\rm s}^{-1}$, $J_{\rm c} = 10^{10}{\rm A/m}^2$,$U_0 = 16k_{\rm B}T$, the sweep rate is $0.01\,{\rm T/s}$, the maximum external magnetic field is $1\,{\rm T}$, which are the same as in Ref.[13]. Using C Programming Language, we obtained the same magnetic moment hysteresis loop (for a zero-field-cooled sample), shown in Fig.1, as in Ref.[13].

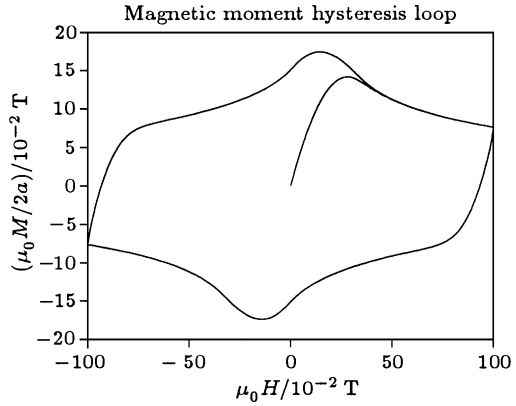


Fig.1. Magnetic moment hysteresis loop calculated by using C programming language. The values for the parameters are as follows: $\omega_0 = 4 \times 10^5\,{\rm s}^{-1}$, $J_{\rm c} = 10^{10}{\rm A/m}^2, U_0 = 16k_{\rm B}T$, altogether 40 pinning centers with a spacing of $x_0 = 5.0 \times 10^{-6}\,{\rm m}$, the sweep rate is $0.01\,{\rm T/s}$, and the maximum external magnetic field is $1\,{\rm T}$.

Ⅲ. COMPUTER SIMULATION ON THE LOCAL FLUX CREEP PROBLEM

A. Hysteresis loops

1. *Low field-sweep rate*

With $\omega_0 = 2 \times 10^6\,{\rm s}^{-1}$, $J_{\rm c} = 10^9\,{\rm A/m}^2$, $U_0 = 16k_{\rm B}T$, altogether 201 pinning centers of a spacing of

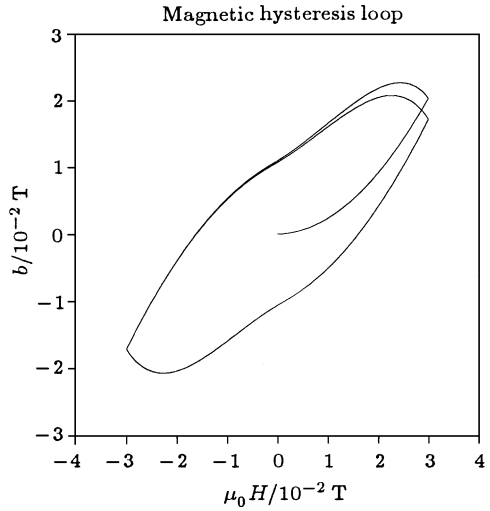


Fig.2(a). Bulk magnetization. The values for the parameters are as follows: $\omega_0 = 2 \times 10^6\,\mathrm{s}^{-1}$, $J_c = 10^9\,\mathrm{A/m}^2, U_0 = 16kT$, altogether 201 pinning centers with a spacing of $x_0 = 5.0 \times 10^{-6}$ m, and the sweep rate is 3×10^{-5} T/s.

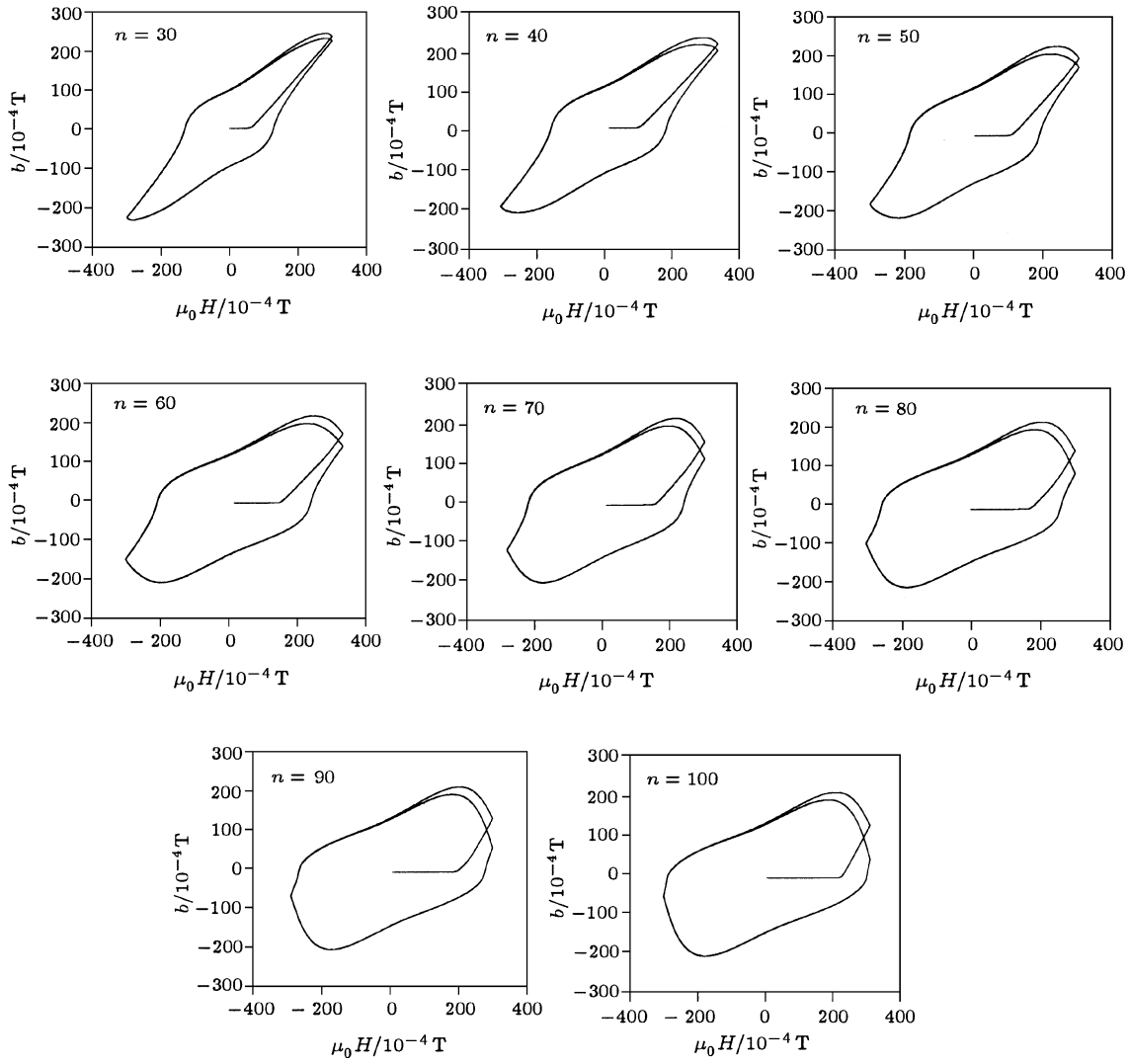


Fig.2(b). Magnetizations at different location of the sample. The values for the parameters are the same as in Fig.2(a).

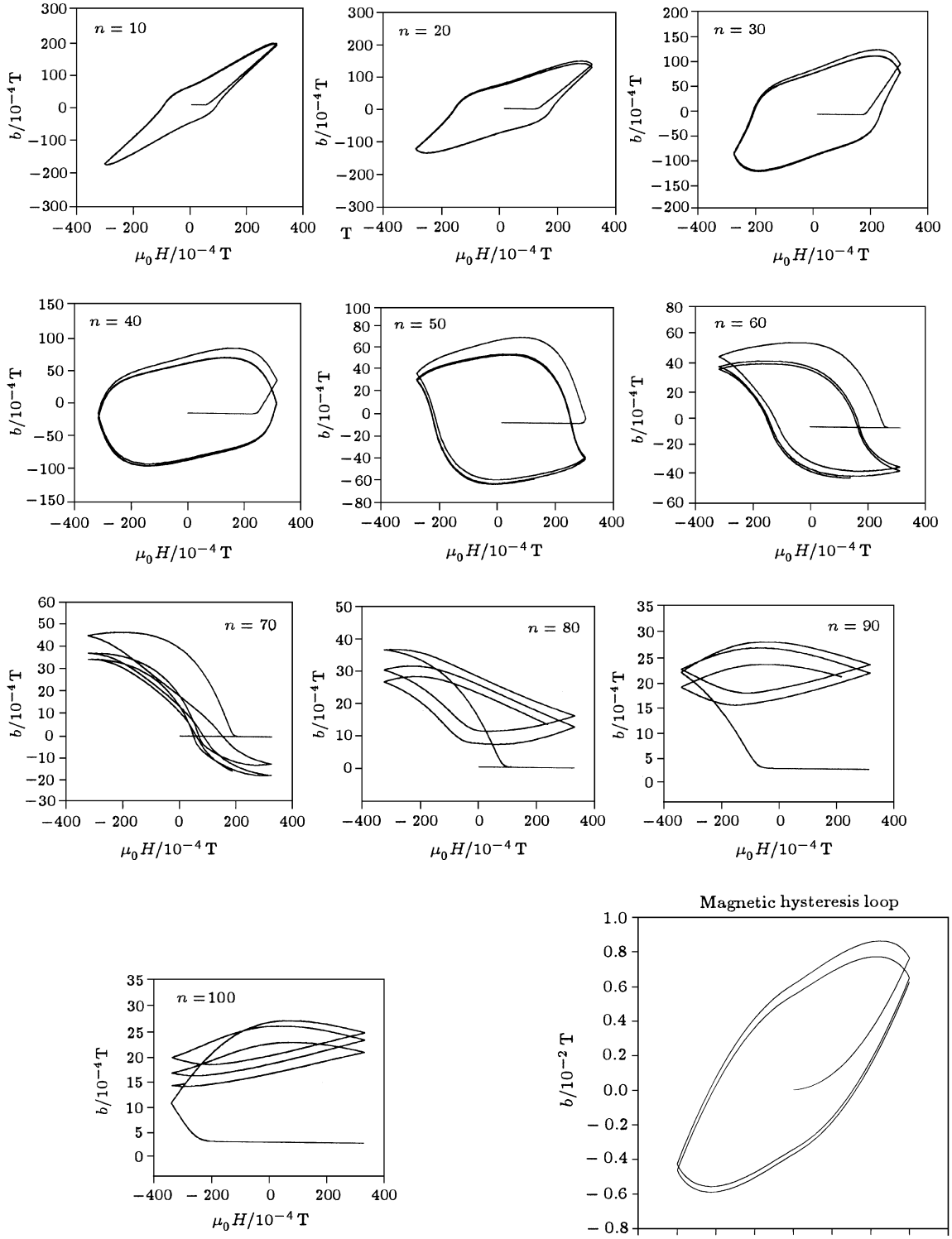


Fig.3(a). Magnetizations at different locations of the sample. The values for the parameters are the same as in Fig.2(a).

Fig.3(b). Bulk magnetizaton. The values for the parameters are the same as in Fig.2, except that the field sweep rate is 3×10^{-4} T/s.

5.0×10^{-6} m, we ramp up the external field at a rate of 3×10^{-5} T/s. The magnetizations of different locations in the sample are shown in Fig.2(b), where $n = 10$ corresponds to the point near the edge, while $n = 100$ the central point. Figure 2(a) shows the bulk magnetization of the whole sample. Both the bulk and local magnetization have two symmetric convexes of varying degree, reflecting the effect of the sign re-

versal of the vortices.[11] Take $n = 20$ as an example, in this figure the external field keeps on decreasing until to the opposite direction. When the number of flux lines within the sample decreases, the activation volume decreases accordingly, and the driving force reduces a little and causes the rate of further leakage of the flux lines to slow down. After the reversal of the applied field, the flux lines of the opposite sign begin to force into the sample and when they reach the point where $n = 20$, the number of the positive vortices will decrease till it is outweighted by the number of negative vortices. It is in this way that the convex is formed. The penetration process can be roughly seen from the series of plots in Fig.2(b).

2. *High field-sweep rate*

Change the external sweep rate into $3\times10^{-4}\,\mathrm{T/s}$. The magnetizations of different locations in the sample are shown in Figs.3(a),3(b), which shows the global magnetization.

Comparison between Figs.2 and 3 shows their notable difference. Because of the relaxation effect of magnetic field penetration, the measurements of hysteresis loop is closely related to the rate and the way of change of the external field. When the applied field is ramped up slowly, there is sufficient time for its change to propagate into the sample, thus enabling the local penetrated magnetic induction B to keep pace with the external field. It is quite different for the quicker ramp-up case, in which the local points cannot keep up with the change of the external field. Qualitatively, the change of the internal field accords with that of the external field except for a phase difference after a certain period of time. In this case, the hysteresis loops can be viewed as Lissajous figures and one can ascertain the relaxation behavior at local points from the orientation of the hysteresis loops.

B. Application of a constant external field

Apply a certain field to the sample instantaneously. A big gradient in the flux density is formed beginning at the surface, so the driving force greatly exceeds the pinning force. The vortices move principally in a viscous -flow way and establish the Bean state which is set up so quickly that it can be viewed as done instantaneously, compared with the slow movement of the flux lines. So in the following simulations, the Bean state serves as the initial state.

1. b-log(t) *curve*

Allow sufficient time for the full penetration of the external field, then remove the field. With $\omega_0 = 2\times10^5\,\mathrm{s^{-1}}$, $J_\mathrm{c} = 1.06\times10^9\,\mathrm{A/m^2}, U_0 = 15k_\mathrm{B}T, \mu_0\mathrm{H}$=0.03 T, altogether 201 pinning centers

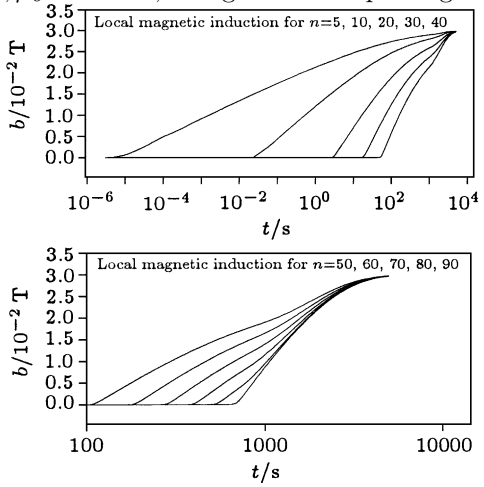


Fig.4. Relaxation of the local magnetic induction at various points during the ramp-up stage. The values for the parameters are as follows: $\omega_0 = 2\times10^5\,\mathrm{s^{-1}}$, $J_\mathrm{c} = 1.06\times10^9\,\mathrm{A/m^2}, U_0 = 15k_\mathrm{B}T, \mu_0\mathrm{H}$=0.03 T, altogether 201 pinning centers with a spacing of $x_0 = 5.0\times10^{-6}\,\mathrm{m}$.

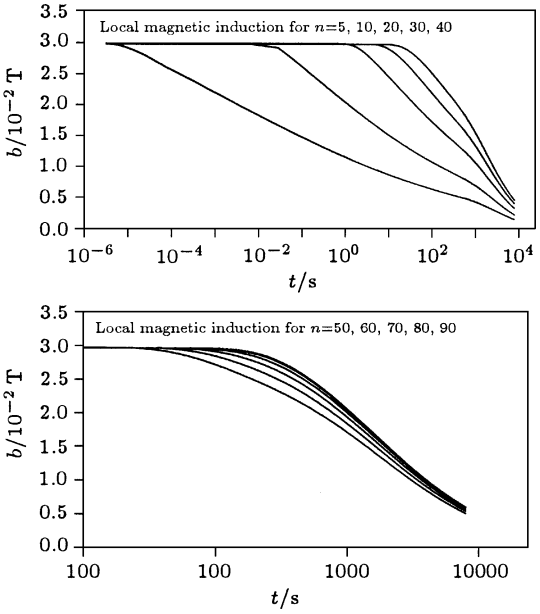


Fig.5. Relaxation of the local magnetic induction at various points after the removal of the external field. The values for the parameters are the same as in Fig.4.

with a spacing of $x_0 = 5.0\times10^{-6}\,\mathrm{m}$, we obtain Figs.4 and 5 which are the b-log(t) graphs for different locations in the sample. Figure 4 shows the penetration condition of local points during ramp-up stage. The speed of penetration is much greater on the edge than in the center. In Fig.5, which shows the local magnetic induction B after the removal of the external field, the behavioral difference between the edge and the center is even more obvious. Closer observation of Figs.4 and 5 will reveal a small bent in both of them. The probable reason for the existence of the bent might

be the penetration speed change, which is caused by the sharp decrease in the driving force due to the convergence of the negative and positive flux lines and its spread from the center to both sides. If we apply a constant field only for a short time and then remove it, the result will be different. For the sake of simplicity, we take $\omega_0 = 2 \times 10^5\,\mathrm{s}^{-1}$, $J_\mathrm{c} = 1.06 \times 10^9\,\mathrm{A/m}^2, U_0 = 15k_\mathrm{B}T, \mu_0\mathrm{H}{=}0.03\,\mathrm{T}$, altogether 61 pinning centers with a spacing of $x_0 = 5.0 \times 10^{-6}\,\mathrm{m}$, as shown in Fig.6. In each of the plot of Fig.6, both the ramp-up and ramp-down processes are calculated and the time is counted separately. The change of the external field can be seen as a square pulse which, owing to the relaxation effect, spreads to the center after such a long time that the internal magnetic field increases even after the external field is removed. And once again we observe that the change of the external field penetrates into the sample quicker in the ramp-up phase than in the ramp-down phase.

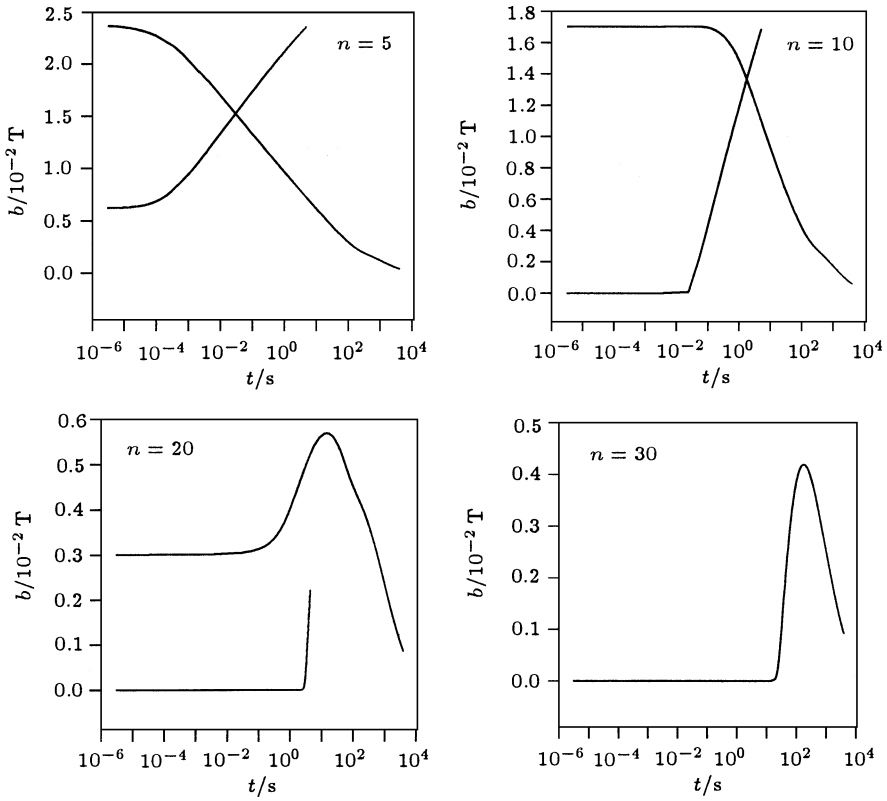


Fig.6. Relaxation of the local magnetic induction at various points after the removal of the external field, which is applied only for a short time. The values for the parameters are as follows: $\omega_0 = 2 \times 10^5\,\mathrm{s}^{-1}$, $J_\mathrm{c} = 1.06 \times 10^9\,\mathrm{A/m}^2, U_0 = 15k_\mathrm{B}T, \mu_0\mathrm{H}{=}0.03\,\mathrm{T}$, altogether 61 pinning centers with a spacing of $x_0 = 5.0 \times 10^{-6}\,\mathrm{m}$.

2. *The penetration speed*

Figure 7 shows the penetration speed of the magnetic field; the vertical axis represents the position of the points in the sample, the horizontal axis corresponds to the time when the external field reaches this point. The values of the parameters are $\omega_0 = 2 \times 10^5\,\mathrm{s}^{-1}$, $J_\mathrm{c} = 1.06 \times 10^9\,\mathrm{A/m}^2, \mu_0\mathrm{H}{=}0.03\,\mathrm{T}$, altogether 201 pinning centers with a spacing of $x_0 = 5.0 \times 10^{-6}\,\mathrm{m}$ .For the shorter line $U_0 = 16k_\mathrm{B}T$, the longer line $U_0 = 18k_\mathrm{B}T$. From this figure one can see that U_0 exerts a great influence on the penetration speed. Information about the sample can be obtained if further fitting is done to the curves.

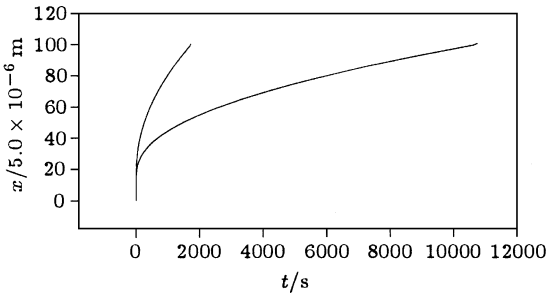


Fig.7. The penetration speed of the magnetic field. The values for the parameters are as follows: $\omega_0 = 2 \times 10^5\,\mathrm{s}^{-1}$, $J_\mathrm{c} = 1.06 \times 10^9\,\mathrm{A/m}^2, \mu_0\mathrm{H}{=}0.03\,\mathrm{T}$, altogether 201 pinning centers with a spacing of $x_0 = 5.0 \times 10^{-6}\,\mathrm{m}$. For the shorter line $U_0 = 16k_\mathrm{B}T$, the longer line $U_0 = 18k_\mathrm{B}T$.

C. The effect of Self-Organized Criticality(SOC)

About ten years ago, Bak, Tang and Wiesenfeld[14] proposed the notion of self-organized criticality dealing with systems with both temporal and spa-

tial degrees of freedom. They discovered that such dynamical systems involve much interaction between individual degrees of freedom and evolve naturally toward a critical state which is very sensitive to outside perturbations. SOC proposes that a nonequilibrium system can organize itself into a certain critical state through its own feedback mechanism, independent of such parameters as temperature in phase transitions, or initial conditions, thus offer a brand-new way of thinking over the spatial and temporal complexities existing in nature. Readers who are interested in SOC theory can refer to Refs.[14–16]. As early as more than thirty years ago, Bean[17] and de Gennes[18] had noted the close analogy between the marginally stable state of vortices in hard superconductors and the marginally stable slope of sand in a sandpile, a typical example for illustrating SOC theory. These early analogies have been used mainly to understand the static distribution of flux in a hard superconductor. Recently, the dynamics of such systems have received much attention. In the case of magnetic field penetration, the effect of SOC equals to reducing the effective activation energy, thus speeding up penetration. As regards the vortex avalanches, some believe they are triggered by thermal activation, some think they happen randomly. In our work, we take the magnitude of the gradient of the magnetic field as a criterion for the occurrence of avalanche, as shown in Fig.8. Figure 8(a) shows the case in which the pinning potential is uniform and there is no SOC mechanism, Fig.8(b) the case that the pinning potential is uniform and there is the SOC mechanism, and Fig.8(c) the case that the pinning potential is nonuniform and there is the SOC mechanism. The parameters are $\omega_0 = 2 \times 10^5\,\mathrm{s}^{-1}$, $J_\mathrm{c} = 3.18 \times 10^9\,\mathrm{A/m}^2$, μ_0H=0.03 T, altogether 61 pinning centers with a spacing of $x_0 = 5.0 \times 10^{-6}\,\mathrm{m}$. For the uniform potential we have $U_0 = 16k_\mathrm{B}T$, for the nonuniform potential $U_0 = (18 \pm 2)k_\mathrm{B}T$. One can note that fluctuations in Fig.8(c) is much greater than that in Fig.8(b) because nonuniform potential can increase the local magnetic gradient and thus causes more notable fluctuations; in all the three plots, fluctuations is more evident in the ramp-up case than in the ramp-down case. What we simulate here is the non-full-penetration case, so when the external field is turned down, the distribution of the internal field is less sharp and results is less fluctuations.

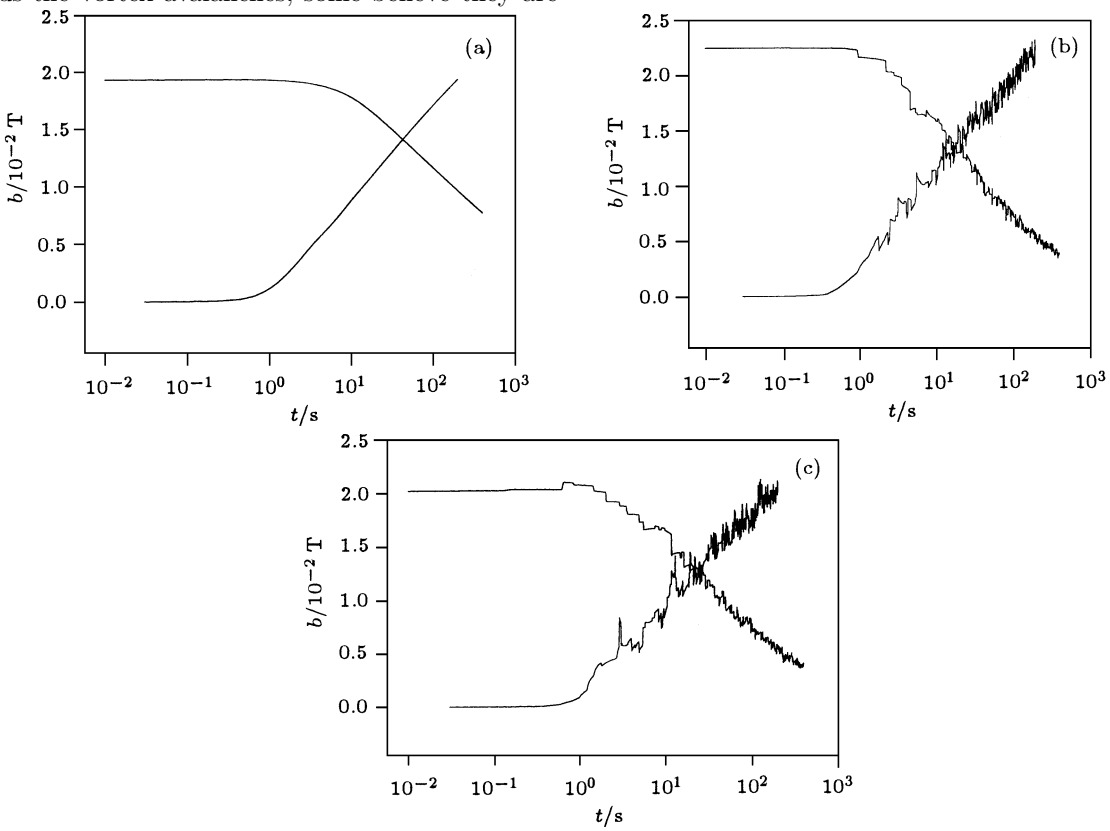


Fig.8. The value for the parameters are as follows: $\omega_0 = 2 \times 10^5\,\mathrm{s}^{-1}$, $J_\mathrm{c} = 3.18 \times 10^9\,\mathrm{A/m}^2$, μ_0H=0.03 T, altogether 61 pinning centers with a spacing of $x_0 = 5.0 \times 10^{-6}\,\mathrm{m}$. (a),(b) and (c) all show the relaxation process in the sample, but represent different conditions: (a) the pinning potential is uniform and there is no SOC mechanism, $U_0 = 16k_\mathrm{B}T$; (b) the pinning potential is uniform and there is SOC mechanism, $U_0 = 16k_\mathrm{B}T$; (c) the pinning potential is nonuniform and there is SOC mechanism, $U_0 = (18 \pm 2)k_\mathrm{B}T$.

IV. CONCLUSIONS

From the above simulations and discussions, we conclude that relaxation effect is the main feature of flux creep and determines the general form of flux distribution; the measurement of hysteresis loops is dependent on field sweep rate; SOC can explain the appearance of fluctuation to some extent; and nonuniform pinning potentials can enhance the fluctuation.

ACKNOWLEDGEMENTS

We are grateful to Prof. H. H. Wen for useful discussions with him and for his critical reading of this article.

REFERENCES

[1] G. Blatter, M. V. Feigel'man, V. B. Geshkenbein, A. I. Larkin and V. M. Vinokur, *Rev. Mod. Phys.*, **66**(1994), 1125.

[2] Y. B. Kim, C. F. Hempstead and A. R. Strand, *Phys. Rev. Lett.*, **9**(1962), 306.

[3] M. V. Feigel'man, V. B. Geshkenbein, A. I. Larkin and V. M. Vinokur, *Phys. Rev. Lett.*, **63**(1989), 2303.

[4] E. Zeldov, N. M. Amer, G. Koren, A. Gupta, R. J. Gambino and M. W. McElfresh, *Phys. Rev. Lett.*, **62**(1989), 3093; *Appl. Phys. Lett.*, **56**(1990), 680.

[5] J. R. Thompson, Y. R. Sun and F. Holtzberg, *Phys. Rev.*, **B44**(1991), 458.

[6] E. Zeldov, A. I. Larkin, V. B. Geshkenbein, M. Konczykowski, D. Majer, B. Khaykovich, V. M. Vinokur and H. Shtrikman, *Phys. Rev. Lett.*, **73**(1994), 1428.

[7] M. V. Feigel'man, V. B. Geshkenbein and V. M. Vinokur, *Phys. Rev.*, **B43**(1991), 6263.

[8] M. R. Beasley, R. Labusch and W. W. Webb, *Phys. Rev.*, **181**(1969), 682.

[9] Y. Abulafia, A. Shaulov, Y. Wolfus, R. Prozorov, L. Burlachkov, Y. Yeshurun, D. Majer, E. Zeldov and V. M. Vinokur, *Phys. Rev. Lett.*, **75**(1995), 2404.

[10] E. H. Brandt, *J. Low Temp. Phys.*, **53**(1983), 41; H. J. Jensen, A. Brass,A. Ch. Shi and A. J. Berlinsky, *Phys. Rev.*, **B41**(1990), 6394; H. J. Jensen, *Phys. Rev. Lett.*, **64**(1990), 3103; O. Pla and F. Nori, *Phys. Rev. Lett.*, **67**(1991), 919.

[11] R. A. Richardson, O. Pla and F. Nori, *Phys. Rev. Lett.*, **72**(1994), 1268.

[12] C. P. Bean and J. D. Lingston, *Phys. Rev. Lett.*, **12**(1964), 14.

[13] H. G. Schnack and R. Griessen, *Phys. Rev. Lett.*, **72**(1994), 1268.

[14] P. Bak, C. Tang and K. Wisenfeld, *Phys. Rev. Lett.*, **59**(1987), 381; *Phys. Rev.*, **A38**(1988), 364.

[15] C. Tang, *Physica*, **A194**(1993), 315.

[16] O. Pla and F. Nori, *Phys. Rev. Lett.*, **67**(1991), 919.

[17] C. P. Bean, *Phys. Rev. Lett.*, **8**(1962), 250.

[18] P. G. de Gennes, Superconductivity of Metals and Alloys (W. A. Benjamin, New York, 1966).